

PAPER • OPEN ACCESS

Nonlinear model parameter analysis of ULFO in large-scale hydropower systems

To cite this article: Kunjun Zhang *et al* 2019 *IOP Conf. Ser.: Earth Environ. Sci.* **227** 032042

View the [article online](#) for updates and enhancements.

Nonlinear model parameter analysis of ULFO in large-scale hydropower systems

Kunjun Zhang^{1,4}, Jian Zhang¹, Guanhong Wang¹, Wenfeng Li¹, Jinmei Gesang² and Dang Jie³

¹ China Electric Power Research Institute, Beijing 100192, China;

² State Grid Tibet Electric Power Co., Ltd;

³ Technology Center of Central China Grid.

⁴ Email: zhangkunjun@163.com

Abstract. The instability of the primary frequency regulation process of hydroelectric units has led to the occurrence of ultra-low frequency oscillations (ULFO) which frequency is less than 0.1 Hz. It mainly appears in the isolated power grid and direct current delivery system with high proportion of hydropower in recent years. So it is very important to study the influence of the main link parameters of the primary frequency regulation on ULFO including the water inertia time constant, system load frequency regulation coefficient. In this paper, a nonlinear model based on each link of primary frequency regulation process is built, and the oscillation frequency of the system under the influence of different parameters is determined by using a variety of frequency domain analysis methods. The influence of the main parameters on the frequency oscillation of the system is analyzed in detail, including the joint stability region which guarantees the stability of the system under the coupling of the governor parallel PID parameters. Nonlinear link is linearized by the method of description function. A new method to determine the parameter range of each link is proposed.

1. Introduction

After years of application and operation, primary frequency regulation plays an important role in the frequency control and in the improvement of power quality. The primary frequency regulation of hydropower is to control the power grid by regulating the frequency-power characteristics of the unit itself. It includes system load frequency regulation and the torque output of the prime mover controlled by the proportional–integral–derivative (PID) controller of the governor. The combined action of them constitutes the effect of primary frequency regulation on the suppression of frequency fluctuation.

In recent years, with the construction of ultra-high voltage direct current (UHVDC) in China's power grid, the abundant hydropower resources of Southwest Power Grid are sent out through UHVDC. But in the actual power grid, the oscillation periods of 10 s and 14 s were observed in island test of Jinping-Sunan DC project and the frequency fluctuation was obvious. The amplitude of fluctuation is $\pm 0.23\text{Hz}$ and $\pm 0.26\text{Hz}$ respectively. The above event is caused by the instability of governor of hydropower plant in DC island power system [1],[2]. Except for the oscillation in small DC islanded power system, when the Southern China Power Grid conducted the Yunnan asynchronous interconnection system characteristic test in March, 2016, the oscillation frequency of Yunnan power grid was 0.05 Hz and the frequency fluctuation was between 49.9 and 50.1 Hz. Figure 1



shows the frequency curve of Yunnan main power grid. Similar ultra-low frequency oscillations have occurred in Burma power grid, Columbia power grid and Turkey power grid[3-5].

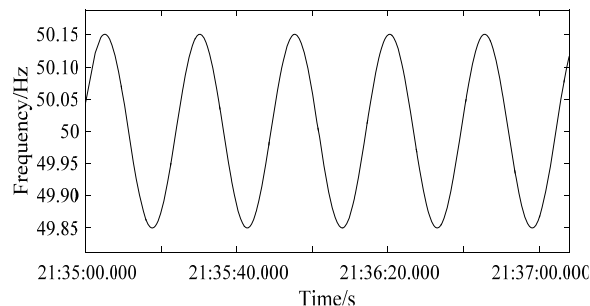


Figure 1. Frequency curve of Yunnan main power grid.

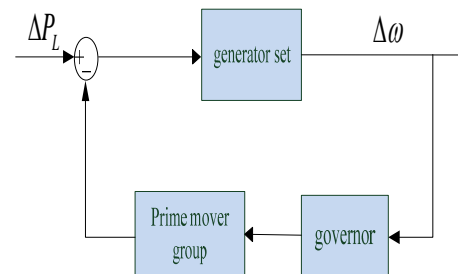


Figure 2. Simplified process diagram of primary frequency regulation

The mechanism of ULFO is different from that of low frequency oscillation caused by relative oscillation between rotors of generator. The oscillation frequency of ultra low frequency oscillation is generally lower than 0.1 Hz, and lower than that of low frequency oscillation frequency in the range of 0.2~2.0Hz. Before the Myanmar, Colombia and Turkey grids, report on ultra-low frequency oscillation appeared in [6]-[8]. The characteristic of ultra-low frequency oscillation is the direction of velocity variation of each unit is the same, and there is no obvious oscillation among the units [9],[10]. The characteristics and conditions of the existing ultra-low frequency oscillation cases are analyzed. It is pointed out that the water hammer effect is one of the key factors that cause the ultra-low frequency oscillation in large scale system [11]. The ultra-low frequency oscillation of Yunnan power grid under asynchronous interconnection mode is suppressed by adjusting the deadbands and PID parameters [12]. The dynamic characteristics of hydraulic turbine governor are introduced in detail [13]-[15]. The dynamic model of hydropower plant is established, the dynamic characteristics in the range of ultra-low frequency oscillation are analyzed, and the effect of governor feedforward control on ultra low frequency oscillation is found out[16]. In the literature [17], a PI governor tuning criterion for the pumped storage hydro plants is proposed which can provide frequency support capacity in island power systems having significant renewable energy resources. In the literature[18],the relationship between the speed governing system stability of one unit and that of the system with parallel operation units was proposed to explain that the high proportion of units with an unstable governing system will lead to system frequency instability. Many articles utilized intelligent algorithms to tune the PID parameters in governors, such as particle swarm optimization[19],[20], genetic algorithm[21],[22] and artificial fish swarm algorithm[23]. Based on the above literatures, the detailed effect of the parameter setting on the oscillation in the speed regulation system needs to be further analyzed.

In this paper, the detailed model of hydraulic turbine system participating in primary frequency regulation process of power grid is studied, and a complete primary frequency regulation process model is established. The influence range of main parameters on ultra-low frequency oscillation is analyzed. The influence of proportion, integral and derivative links on oscillation under parallel PID control is studied. The idea of segmental control of PID controller to eliminate the effect of water hammer is proposed.

2. Mathematical model

Figure 2 shows the block diagram of the primary frequency regulation process of power system, which is mainly the process of the speed regulation of the generator by the governor and the prime mover. In this paper, the problem of ultra-low frequency oscillation in primary frequency regulation process is

studied by means of small disturbance stability analysis of the dynamic process. First of all, some models used in the analysis of this paper are briefly described.

2.1. Generator inertial link

The inertia of hydraulic turbine refers to the kinetic energy stored in the rotor itself by the generator rotor at rated speed. The damping coefficient of the generator changes with the state of the system when the system is running, but in the case of small disturbance of the system, the speed of the generator has little change, and the damping winding coefficient is very small compared with the inertia time constant and load-damping constant of the generator. For the sake of simplification, the damping coefficient is considered as a definite value. The rotor operation equation of generator set is as follows:

$$2H \frac{d\Delta\omega}{dt} = \Delta T_m - \Delta T_e - D\Delta\omega \quad (1)$$

H is the inertia time constant of the generator unit, D is the damping coefficient of the generator unit, ΔT_m is the mechanical torque change of the generator unit, ΔT_e is the electromagnetic torque change of the generator unit. Because of the small disturbance in the system similarly, the speed of the generator unit has little change, and $\omega=1$ can be considered approximately. Mechanical power variation of generating units ΔP_m and per unit of ΔT_m can be considered approximately equal. Same argument, electromagnetic power variation of generating units ΔP_e and per unit of ΔT_e are equal, so that the formula (1) can be rewritten as:

$$2H \frac{d\Delta\omega}{dt} = \Delta P_m - \Delta P_e - D\Delta\omega \quad (2)$$

When the frequency changes, system load power regulation variation is ΔP_L .

$$\Delta P_L = K_L \Delta f \quad (3)$$

When the load disturbance occurs, the electromagnetic power in the whole power grid has the same change at the same time.

$$\Delta P_e = \Delta P_L \quad (4)$$

To substitute formula (1) and (2) in form (3) can be obtained.

$$2H \frac{d\Delta\omega}{dt} = \Delta P_m - K_L \Delta f - D\Delta\omega \quad (5)$$

The inertia time constant of the system is determined by the following formula:

$$H_{eq} = \sum_{i=1}^N H_i \cdot S_i / S_{total} \quad (6)$$

For large power grid, H_{eq} is the equivalent inertial time constant. Where N is the number of all generators in the large power grid and H_i is the inertia time constant of the generator i and S_i is the rated capacity of the generator i and S_{total} is the sum of the installed capacity of all generators in the large power grid. Taking the two-machine system as an example, suppose the inertia time constant of the first generator is H_1 , the capacity is S_1 , the inertia time constant of the second generator is H_2 , and the capacity is S_2 . Figure 3 shows the block diagram of its equivalent transfer function.

$$H_{eq} = (H_1 \cdot S_1 + H_2 \cdot S_2) / (S_1 + S_2) \quad (7)$$

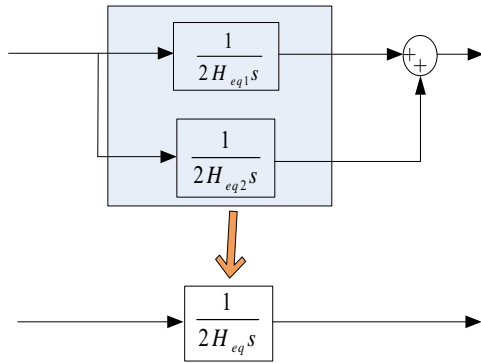


Figure 3. Parallel equivalent transfer function of generator set.



Figure 4. Basic structure of hydraulic turbine governing system.

$$H_{eq1} = (S_1^2 H_1^2 - S_2^2 H_2^2) / S_1 S_{total} H_1 \tag{8}$$

$$H_{eq2} = (S_2^2 H_2^2 - S_1^2 H_1^2) / S_2 S_{total} H_2 \tag{9}$$

By observing formula (8) and formula (9), we can get that there must be one negative value in H_{eq1} and H_{eq2} , and its physical meaning is: in two machine systems, if the parameters of two generators are not identical, then the inertial time constant (H_{eq}) of the system must be a number between H_1 and H_2 . The negative values in H_{eq1} and H_{eq2} indicate that the inertial time constant of this machine is smaller than that of the system. This generator was "towed" by another generator, whereas the positive values in H_{eq1} and H_{eq2} indicate that the inertial time constant of this machine is larger than the inertial time constant of the system. This generator is "towing" another generator. In the multimachine system, the above conclusions can also be applied. In this paper, for the sake of simplification, the inertia time constant of power grid is set to H_{eq} .

2.2. Hydraulic turbine governing system model

The hydraulic turbine governing system model consists of the governor model and the turbine prime mover model. Figure 4 shows basic structure of hydraulic turbine governing system. There are many types of governor model, such as mechanical hydraulic type, parallel PID primary electro-hydraulic servo system. As long as the governor model with similar principle and structure is selected, the actual characteristics of the control system can be reflected more truthfully. The ideal hydraulic turbine model is used in the prime mover, which is a linearized model near the equilibrium point, and it is suitable for the analysis of small disturbance stability.

2.2.1. Hydraulic turbine mathematical model. The turbine adopts ideal mathematical model and linearizes at the stable operating point, which can meet the requirement of small disturbance stability analysis. The relation between turbine guide blade opening and mechanical power is obtained by Laplace transformation as follows. Derivation is from [1].

$$\frac{\Delta P_m}{\Delta y} = \frac{W_1(s)}{W_2(s)} = \frac{(1 - T_w s)}{(1 + 0.5 T_w s)} \tag{10}$$

Where, Δy is the opening variation of guide vane, T_w is the water inertia time constant, and it is defined as:

$$T_w = \frac{L U_0}{a_g H_0} \tag{11}$$

In the formula, a_g is the gravity acceleration ;L is the length of the penstock; U is the flow velocity

equivalent transfer function is introduced before the parameter root trajectory is drawn. The closed-loop characteristic equation of the system is as follow.

$$1 + G_k(s) = 1 + E(s)H(s) = 0 \tag{14}$$

For the variable parameter A to be studied in the open-loop transfer function, the following transformation can be made for the above formula:

$$Q(s) + AP(s) = 1 + E(s)H(s) = 0 \tag{15}$$

According to the above formula, the equivalent unit feedback system can be obtained, and its equivalent open-loop transfer function is:

$$D_1(s)H_1(s) = A \frac{P(s)}{Q(s)} \tag{16}$$

Based on the actual parameters of the hydro-generating unit, the parameter root locus under the change of parameter A can be drawn, and the influence of time constant range of each link on the stability of oscillation can be discussed. The calculated parameters are listed in table 1.

Table 1. Model parameters.

The parameter name	Symbol	The parameter value
Moment of inertia of generator	2H _{eq}	8
Damping coefficient of generator	D _{eq}	0.3
Load frequency regulation coefficient	K _L	1.7
The water inertia time constant	T _w /s	3
The proportional coefficient of the derivative link	T _D /s	0.01
The time constant of the servo system	T _G /s	0.5
Proportion gain	K _p	3
Integral gain	K _i	0.4
Derivative gain	K _d	0.3
Permanent speed droop	BP/%	4
Negative direction of the deadbands	-DB1	0.05
Positive direction of the deadbands	DB1	0.05

3.1. Influence of unit time constant on oscillation frequency

The unit's inertial time constant can refer to the definition of the generator inertial time constant. The higher its value is, the slower its rotor speed changes for the same torque, and the stronger the damping effect for the oscillation. When the effect of 2H_{eq} on ultra-low frequency oscillations is studied separately, its equivalent open-loop transfer function is as follows:

$$G_{k1}(s) = \frac{B(s)D(s)G(s)W_2(s) + K(s)W_1(s)}{(D_{eq} + K_L)B(s)D(s)G(s)W_2(s) + K(s)W_1(s)} \times 2H_{eq} \tag{17}$$

Figure 6 shows the corresponding generalized root locus. According to the determination of the parameter range for the stability of the system by the generalized root locus, the inertial time constant of the unit to ensure the stability of the system is greater than 7.58s. If the inertial time constant of the unit takes the critical stability value, the unit step response of the system is equal amplitude oscillation, figure 7 shows unit step response of different time constants. At this point, it can be considered that the total damping provided by the whole system is zero. At this point, if the system bird chart is drawn,

the intersection point of the amplitude-frequency characteristic curve and the horizontal axis is the ultra-low frequency oscillation frequency of the system, ω_c and the oscillation frequency is 12.59s. When the value of 2Heq is 7s and 8s, the corresponding oscillation periods are 12.101s and 12.887s respectively. According to the relationship between the unit time constant and the oscillation frequency obtained from the time domain simulation, it can be seen that the increase of the value of 2Heq is conducive to the frequency stability of the unit, and the larger the value, the smaller the frequency of the ultra-low frequency oscillation.

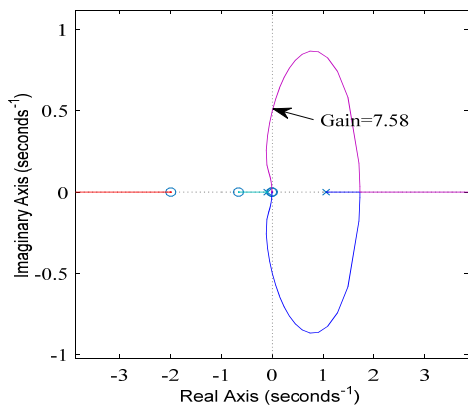


Figure 6. Root locus of the unit time constant as variable.

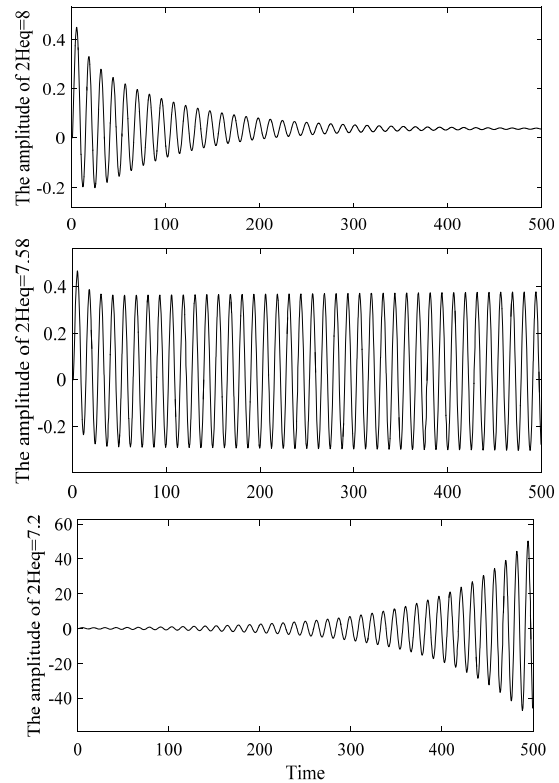


Figure 7. Unit step response of different time constants.

3.2. Influence of the water inertia time constant on oscillation frequency

In the literature [2], the ultra-low frequency oscillation problem in the asynchronous connection process of Yunnan power grid are analyzed. In the analysis of PMU data results, it is found that in the case of frequent adjustment of the blade opening of the turbine, the reverse regulation effect of the water hammer has a significant negative impact on the dynamic stability and response characteristics of the system. Therefore, it is necessary to make a detailed analysis of the influence of water start-up time on the system oscillation frequency. Figure 8 shows the corresponding generalized root locus.

When the water inertia time constant T_w is a variable, the equivalent open-loop transfer function of the system is:

$$G_{k2}(s) = \frac{s[0.5B(s)D(s)G(s)T(s) - K(s)]}{B(s)D(s)G(s)T(s) + K(s)} \times T_w \tag{18}$$

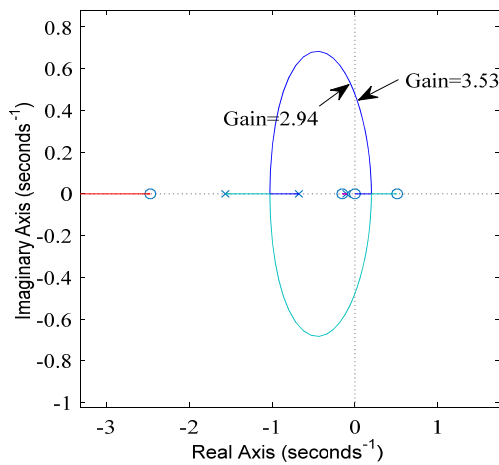


Figure 8. The root locus of the water inertia time constant.

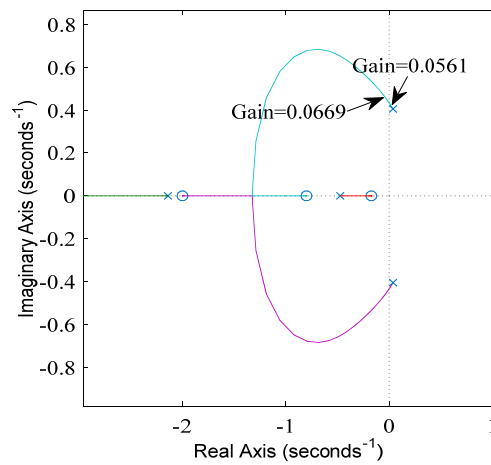


Figure 9. Root locus of permanent speed droop as variable.

Figure 8 shows the root locus of the water inertia time constant. The water inertia time constant which guarantees the critical system stability is between 2.94 s and 3.53s. According to the definition of T_w , it is known that the value is related to the length of the penstock, the steady value of the flow velocity and the head height of the guide vanes, which are difficult to control in actual hydropower plant operation. The small variation of T_w has obvious effect on stability. In the case of zero damping, the value of T_w is 3.132s and the oscillation frequency of the system is 0.0763Hz.

3.3. The influence of permanent speed droop coefficient on the oscillation frequency

The constant of permanent speed droop (B_p) of hydroelectric generating set is defined as the opposite number of the slope between the relay stroke of the actuator and the speed curve of the turbine. Its specific value is set according to the governor and does not change with the working condition after setting. The depth of primary frequency regulation of hydropower unit is inversely proportional to B_p , and the smaller the value is, the greater the power of primary frequency regulation is shared by the corresponding unit. Therefore, it is necessary to study the effect of the parameter range on the ultra-low frequency oscillation.

When studying B_p , the equivalent open loop transfer function of the system is:

$$G_{k3}(s) = \frac{K_t D(s) G(s) T(s) W_2(s)}{s D(s) G(s) T(s) W_2(s) + K(s) W_1(s)} \tag{19}$$

Figure 9 shows the root locus of permanent speed droop coefficient. In view of the above parameters, the critical stability value of the permanent speed droop is between 0.0561 and 0.0669. The closed-loop characteristic equation is given as follows:

$$B(s) = (s + B_p K_t)(1 + T_G s)(2H_{eq} s + D)(1 + 0.5T_w s)(1 + T_D s) + [(1 + T_D s)sK_p + s^2 K_D + (1 + T_D s)K_t](1 - T_w s) = 0 \tag{20}$$

Let $s = j\omega$, the characteristic equation is written as the form of real and imaginary parts: $B(s) = P(\omega) + Q(j)$, make each of them zero, the critical constant slip coefficient is 0.0639 and the oscillation frequency is 0.433 Hz. It can be seen from the root locus that when B_p is larger than the critical value, the damping of the system is positive and tends to be stable, and the larger the value, the greater the oscillation frequency.

3.4. Influence of PID controller parameters on oscillation frequency

PID controller parameters have obvious influence on system performance indexes such as overshoot, stability, regulation speed and steady-state error. When the system is in the ascending phase, the larger

value of proportional gain(Kp) and the smaller value of differential gain(Kd) can make the system have better tracking performance. When the system overshoot, it is necessary to select a smaller Kp and integral gain(Ki) value. When the system tends to be stable, the PID parameter can also be adjusted to eliminate the steady-state error [1]. The analysis of the effect of Kp, Ki, Kd on the ultra-low frequency oscillation produced in the above primary frequency regulation model can provide an effective means to suppress the oscillation.

Taking Kp, Ki and Kd as variables, the corresponding equivalent open-loop transfer function is:

$$\begin{aligned}
 G_{k4}(s) &= \frac{D(s)W_1(s)s \times K_p}{B(s)D(s)G(s)T(s)W_2(s) + s^2 K_d + D(s)K_i W_1(s)} \\
 G_{k5}(s) &= \frac{D(s)W_1(s) \times K_i}{B(s)D(s)G(s)T(s)W_2(s) + s^2 K_d + D(s)K_i W_1(s)} \\
 G_{k6}(s) &= \frac{s^2 W_1(s) \times K_d}{B(s)D(s)G(s)T(s)W_2(s) + (sK_p + K_i)D(s)W_1(s)}
 \end{aligned}
 \tag{21}$$

In order to avoid the coupling effect of Kp, Ki, Kd in the process of regulation, the other two variables can be set to zero when one of the variables is studied separately, figure 10-12 show the generalized root locus corresponding to Kp, Ki and Kd.

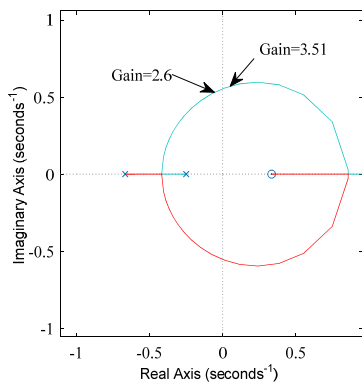


Figure 10. The root locus of Kp .

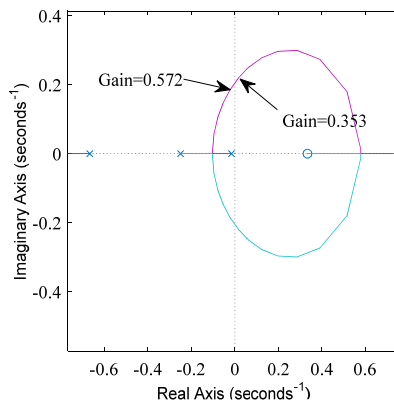


Figure 11. The root locus of Ki.

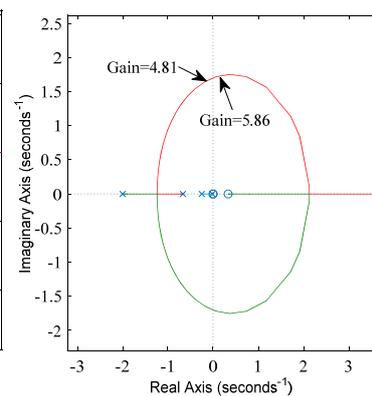


Figure 12. The root locus of Kd.

The critical stable value of Kp is 3.385, the corresponding oscillating angular frequency is 0.555rad/s. The value of Kp decreases and the oscillation frequency decreases. The critical stable value of Ki is 0.488, the corresponding oscillating angular frequency is 0.210rad/s. The smaller value of Ki is, the bigger value of oscillation frequency is.

The critical stability value of Kd is 5.5825, and the corresponding oscillation angular frequency is 1.684rad/s. The value of Kd decreases and the oscillation frequency decreases, also. In summary, the smaller the value of Kp, Ki and Kd, the greater the stability margin of the system. Due to the existence of slip coefficient, Kp, Ki and Kd have coupling effects on oscillation. The joint stability region of PID control parameters is obtained by using Routh criterion to observe the corresponding PID parameters in the stable system.

Figure 13,14 show the PID parameter stability region. For the model parameters used in the simulation, the PID parameter set in the stable region can meet the system stability requirements. It can be seen that the selection of boundary PID parameter sets corresponds to the critical stable state of the system. In addition, the stability of the system can be further studied by the internal parameters of the stability domain. The ultra-low frequency oscillation caused by water hammer effect is suppressed

by selecting parameter groups in different performance regions.

It can be seen from the stability region of the Kp-Kd plane that the value of Kd corresponds to 5.6 and the value of Kp is about 3.4 at the boundary of Kp and Kd axis, that is to take Kp=0 and Ki=0. It coincides with the effect of single argument studied earlier.

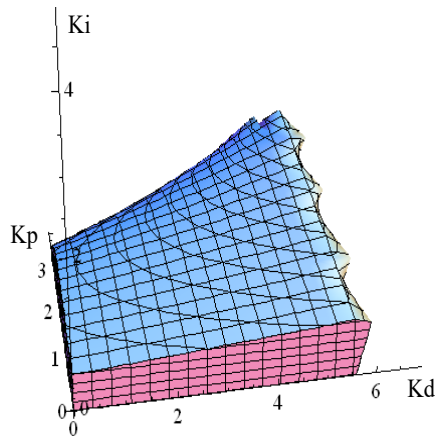


Figure 13. Stable region of the global Kp-Ki-Kd plane.

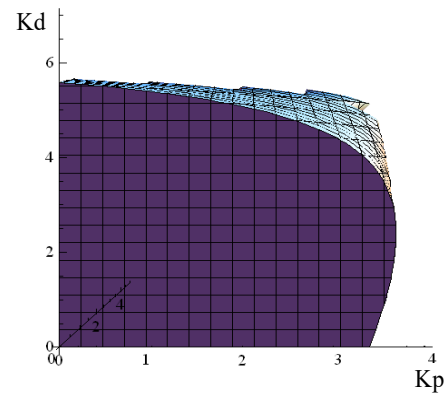


Figure 14. Stability region of Kp-Kd plane.

3.5. Influence of load regulation coefficient on Oscillation Frequency

The self-regulating coefficient of load to frequency has the same damping effect on frequency deviation as the damping coefficient of generator in actual power system. Because the value of D_{eq} in actual unit is usually very small, their influence on ultra-low frequency oscillation can be analyzed in a unified way. Figure 15 shows the corresponding generalized root trajectories.

Let $D=K_L+D_{eq}$, for the case of D , the equivalent open loop transfer function of the system is:

$$G_{K6}(s) = \frac{B(s)T(s)G(s)W_2(s)}{2H_{eq}B(s)T(s)G(s)W_2(s)s + K(s)W_1(s)} \times D \tag{22}$$

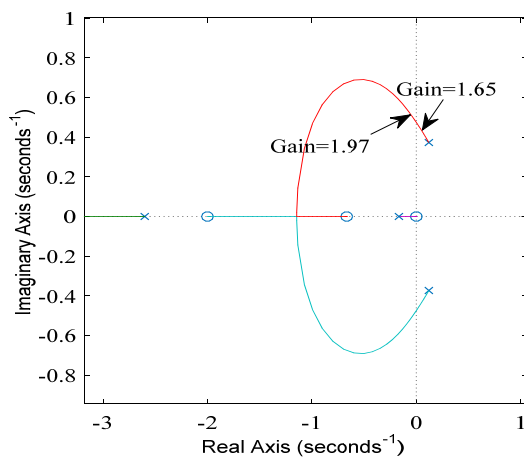


Figure 15. Root locus of load regulation coefficient as variable.

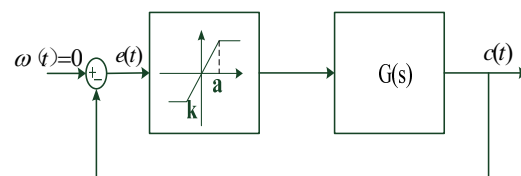


Figure 16. Control system with Limiters characteristics.

The critical stability value is 1.835 and the oscillation angular frequency is 0.481rad / s by calculating the traversing frequency of its amplitude-frequency characteristic. The larger the value, the greater the oscillation frequency.

4. Linearization of nonlinear links

The method of describing function can be used to analyze the stability and self-oscillation of nonlinear systems without external action. It can not be restricted by the order of the system. Next, the deadbands and the limiters of the model are analyzed by the descriptive function method.

4.1. Description function of the deadbands and limiters

For a nonlinear element, its input and output functions can be described as $y = f(x)$, where the input signal is a sinusoidal signal $x(t) = A \sin \omega t$. Harmonic analysis of steady state output $y(t)$ of nonlinear link is carried out. Generally, it is a nonlinear periodic signal, which can be expanded into Fourier series:

$$y(t) = A_0 + \sum_{n=1}^{\infty} (A_n \cos \omega t + B_n \sin \omega t) = A_0 + \sum_{n=1}^{\infty} Y_n \sin(n \omega t + \varphi_n) \quad (23)$$

In the formula, A_0 is the direct current component and $Y_n \sin(n\omega t + \varphi_n)$ is the n th harmonic component. If $n > 1$, Y_n is very small, that is, the nonlinear part can be considered to have the similar frequency response form as the linear part. Therefore, the description function of the nonlinear link is defined as the plural ratio of the first harmonic component in the steady-state output and the sinusoidal input signal, which is expressed by $M(A)$. That is,

$$M(A) = |M(A)| e^{j\varphi_1} = \frac{Y_1}{A} e^{j\varphi_1} = \frac{B_1 + jA_1}{A} \quad (24)$$

The static characteristics of the deadbands and limiters are shown. The description function of the deadbands is expressed as

$$M_1(A) = \frac{2K}{\pi} \left[\frac{\pi}{2} - \arcsin \frac{\Delta}{A} - \frac{\Delta}{A} \sqrt{1 - \left(\frac{\Delta}{A}\right)^2} \right], \quad A \geq \Delta \quad (25)$$

The description function of the limiters is

$$M_2(A) = \frac{2K}{\pi} \left[\arcsin \frac{a}{A} + \frac{a}{A} \sqrt{1 - \left(\frac{a}{A}\right)^2} \right], \quad A \geq a \quad (26)$$

4.2. Influence of limiters

The limiters is an important part of the governor's performance. In the dynamic process of frequency change, once the output of the PID controller reaches the upper limit of the limiters, the output power of the prime mover reaches the maximum value, and no longer responds to the change of frequency drop. Similar to the deadbands, the limiters can also be equivalent to a change gain, whose value range is 0-k. Figure 16 shows the primary frequency control system with saturation nonlinearity.

According to formula (25), it takes $u = a/A$ and derivation to $M_1(u)$.

$$\frac{dN(u)}{du} = \frac{4k}{\pi} (1-u^2)^{1/2} \quad (27)$$

When $A > a$, $u = a/A < 1$, so there is $N(u)/du > 0$. $N(u)$ is an increasing function of u . $-1/N(A)$ is the decreasing function of A . Using the descriptive function method, when the nonlinear characteristic is approximately equivalent by the descriptive function method, the characteristic equation of the closed-loop system is as follows:

$$1 + N(A)G(j\omega) = 0, \quad G(j\omega) = -\frac{1}{N(A)} \quad (28)$$

Where $-1/N(A)$ is called a negative backward description function. According to Nyquist criterion, when plotting $-1/N(A)$ and $G(s)$ on the plural plane, if the curve has no intersection point, it shows that formula (27) has no positive real solution. If the point $(R_c(-1/N(A)), I_m(-1/N(A)))$ is surrounded by curve $G(j\omega)$, then the system will be unstable, and A will increase and the system will eventually fail. On the contrary, the system is stable, A will be reduced to zero or the input of the non-linear link to a certain value, or in a small range of fixed value. For a given value of $k=4$, $a=0.5$. Figure 17 shows the curve of $G(j\omega)$ and $-1/N(A)$.

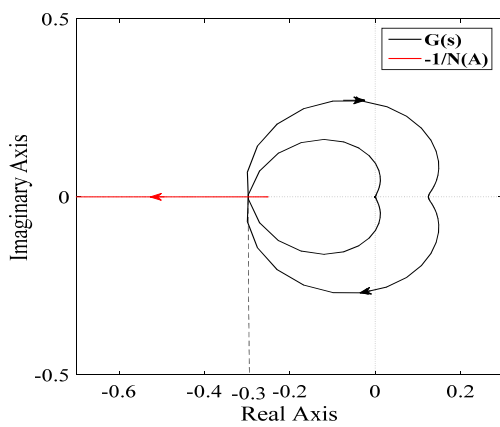


Figure 17. Nyquist diagram of $G(j\omega)$ and $-1/N(A)$.

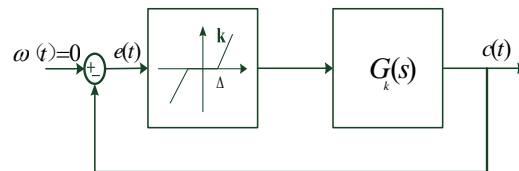


Figure 18. Control system with the deadbands characteristics.

Curves $G(j\omega)$ and $-1/N(A)$ have intersections $(-0.3, j0)$ and at this point, the curve of $-1/N(A)$ increases along the direction of A from the unstable region into the stable region, and there is periodic motion at the intersection point. According to formula

$$\text{Im}[G(j\omega)N(A)] = \text{Im}[G(j\omega)]N(A) = 0, \quad \text{Re}[G(j\omega)N(A)] = \text{Re}[G(j\omega)]N(A) = -0.3 \quad (29)$$

The amplitude $A=0.715$ under oscillation is obtained, that is, the input signal amplitude of the nonlinear link which guarantees the stability of the system is less than this value, and the system tends to be stable.

4.3. Impact of the deadbands

In addition to being affected by the nonlinear characteristics of the limiters, the nonlinear characteristics of the deadbands make the gain of the input in the range of deadbands zero, which is equivalent to the open-loop state. At this time, the system has no adjusting effect and the output of the system is later in time, which reduces the tracking accuracy. On the other hand, when the system is near the steady state, the deadbands range can reduce the effect of the disturbance signal. In addition, it is found that the deadbands can increase the damping of the system and reduce the overshoot of the dynamic process. The existence of the deadbands makes the equivalent gain of nonlinear characteristics change dynamically with the input between $0-k$. When the input is larger than the deadbands range, the equivalent gain of the system becomes larger and the system becomes faster. Conversely, when the system oscillation is weakened, the gain can be reduced and the overshoot will decrease. Figure 18 shows the first frequency regulation control system with saturation nonlinearity.

The amplitude $A = 0.151$ is obtained when $k = 4$, $\Delta = 0.02$, that is, the input signal amplitude of the nonlinear link which guarantees the stability of the system is less than this value, and the system tends to be stable.

5. Conclusions

Based on the modeling and analysis of the model parameters of each link in the process of primary frequency regulation of hydraulic turbines, the oscillation frequency and parameter setting range of the system under the influence of various parameters are determined by using various frequency domain analysis methods. The influence of the main parameters on the frequency oscillation of the system is analyzed in detail, including the joint stability region of parallel PID parameters of the governor to ensure the stability of the system. Through the analysis of descriptive function method, the nonlinear part of the system is simplified, and the deadbands and amplitude limiting parameter tuning to ensure the frequency stability of the system is studied in detail.

Acknowledgment

The research is supported by technology projects of State Grid Tibet Electric Power Co., Ltd ‘Study on Ultra low Frequency Oscillation suppression Technology based on additional damping Controller of hydraulic Turbine Speed Regulation side in Tibet Power Grid’; technology projects of Technology Center of Central China Grid ‘Study on coordination frequency control Technology based on conventional source, pumped-hydro energy storage and new source’.

References

- [1] Chen Yiping, Cheng Zhe, Zhang Kun, et al. 2013 Frequency regulation strategy for islanding operation of HVDC[J] *Proceedings of the CSEE* **33**(4) 96-102
- [2] HE Jingbo, ZHANG Jianyun, LI Mingjie, et al. 2013 An approach for analysis and control of governor stability in islanded HVDC sending system [J] *Proceedings of the CSEE* **33**(16) 137-143
- [3] Gencoglu C 2010 Assessment of the effect of hydroelectric power plants’governor settings on low frequency interarea oscillations [D] *Ankara, Turkey: Middle East Technical University*
- [4] Villegas HN 2011 Electromechanical oscillations in hydro-dominant power systems: an application to the Colombian power system *Digital Repository*
- [5] Cebeci ME, Karağaç U, Tör OB, Ertas A. The effects of hydro power plants’ governor settings on the stability of Turkish power system frequency. Available:http://www.emo.org.tr/ekler/ad6635f33710af6_ek.pdf.
- [6] Villegas Hn 2011 Electromechanical oscillations in hydro-dominant power systems: an application to the Colombian power system *Digital Repository*
- [7] Cebeci ME, Karağaç U, Tör OB, Ertas A. The effects of hydro power plants’ governor settings on the stability of Turkish power system frequency. Available:http://www.emo.org.tr/ekler/ad6635f33710af6_ek.pdf.
- [8] Saarinen L, Norrlund P, Lundin U, Agneholm E, Westberg A 2016 Full-scale test and modelling of the frequency control dynamics of the Nordic power system *IEEE Power Energy Soc General Meet (PESGM)* **2016** 1–5
- [9] Zhou Jinghao, Jiang Chongxi, Gan Deqiang, et al. 2017 Stability analysis of ultra-low frequency oscillation of Yunnan power grid based on value set approach *Power Syst Technol* **41**(10) 3147-52
- [10] Rimorov D, Kamwa I, Joós G 2016 Quasi-steady-state approach for analysis of frequency oscillations and damping controller design *IEEE Trans Power Syst* **31** 3212–20
- [11] Wang Guanhong, Yu Zhao, Zhang Yi, et al. 2016 Characteristics and Analysis of Ultra-low Frequency Oscillation Mode in Power System [J] *Power System Technology* **40** (8) 2324-2329
- [12] Zhang Jianxin,Liu Chunxiao,Chen Yiping et al. 2016 Counter measures and Experiments on

- Ultra-Low Frequency Oscillation of Yunnan Power Grid in Asynchronous Interconnection Mode[J] *Southern Power Grid Technology* **10**(07) 35-39
- [13] Kundur P 1994 Power system stability and control. New York, NY, USA: McGraw-Hill
- [14] IEEE recommended practice for preparation of equipment specifications for speed-governing of hydraulic turbines intended to drive electric generators. IEEE Std125–2007 (Revision of IEEE Std 125–1988); 2007. p. c1–51.
- [15] F P de Mello, R J Koessler 1992 Hydraulic turbine and turbine control models for system dynamic studies *IEEE Transactions on Power Systems* **7** 167–79
- [16] Pico HV, McCalley JD, Angel A, Leon R, Castrillon NJ 2012 Analysis of very low frequency oscillations in hydro-dominant power systems using multi-unit modeling *IEEE Trans Power Syst* **27** 1906–15
- [17] Martínez-Lucas G, Sarasúa JI, Sánchez-Fernández JÁ, Wilhelmi JR 2016 Frequency control support of a wind-solar isolated system by a hydropower plant with long tail-race tunnel *Renew Energy* **90** 362–76. 2016/05/01
- [18] Mo W, Chen Y, Chen H, Liu Y, Zhang Y, Hou J, et al. 2017 Analysis and measures of ultra-low-frequency oscillations in a large-scale hydropower transmission system *IEEE JEmerging Selected Topics Power Electron* 1-1
- [19] Zwe-Lee G 2004 A particle swarm optimization approach for optimum design of PID controller in AVR system *IEEE Trans Energy Convers* **19** 384–91
- [20] Rosen S, Arunagirinathan P, Jayawardene I, Venayagamoorthy GK 2016 Optimal tuning of governors on synchronous generators in a multi-area power system with a large photovoltaic plant *IEEE PES PowerAfrica* **2016** 246–50
- [21] Lansberry JE, Wozniak L 1994 Adaptive hydrogenerator governor tuning with a genetic algorithm *IEEE Trans Energy Convers* **9** 179–85
- [22] Singh MK, Naresh R, Gupta DK 2013 Optimal tuning of temporary droop governor of hydro power plant using genetic algorithm *Int Conf Energy Efficient Technol Sustain* **2013** 1132–7
- [23] Sun X, Fang H 2016 Speed governor PID gains optimal tuning of hydraulic turbine generator set with an improved artificial fish swarm algorithm *IEEE Int Conf Inf Automation (ICIA)* **2016** 2033–5